Int. J. Multiphase Flow Vol. 13, No. 4, pp. 565–575, 1987
Printed in Great Britain.

0301-9322/87 $3.00 + 0.00

STRATIFIED GAS–LIQUID FLOW IN DOWNWARDLY INCLINED PIPES

P. ANDREUSSI
University of Pisa, 56100 Pisa, Italy

L. N. PERSEN
University of Trondheim, Trondheim-NTH, Norway

(*Received* 23 *September* 1985; *in revised form* 15 *October* 1986)

Abstract—Measurements of liquid hold-up and pressure drop are reported for stratified flow in a slightly inclined (0.65° and 2.1°), 5 cm pipeline. Velocity profiles in the gas phase have been determined for a limited number of flow conditions. Semi-empirical correlations are proposed for the transition to slug flow, the interfacial friction factor and the liquid hold-up.

INTRODUCTION

Stratified gas–liquid flow in horizontal or near-horizontal pipes has been widely studied in the past years and a number of models or design equations are now available which represent a substantial improvement with respect to the empirical approach adopted by Lockhart & Martinelli (1949).

Many of the available mathematical models or design methods (Johanessen 1972; Taitel & Dukler 1976; Persen 1984) are based on 1-D momentum balances in the gas and the liquid phases:

$$-A_L\left(\frac{dP}{dx}\right) - \tau_{WL}P_L + \tau_i S_i + \rho_L A_L g \sin\theta = 0 \quad [1]$$

and

$$-A_G\left(\frac{dP}{dx}\right) - \tau_{WG}P_G - \tau_i S_i + \rho_G A_G g \sin\theta = 0, \quad [2]$$

where (dP/dx) is the pressure gradient, A is the phase cross-sectional area, ρ is the density, S is the interfacial width, P is the perimeter over which the stress acts, τ is the shear stress, g is the

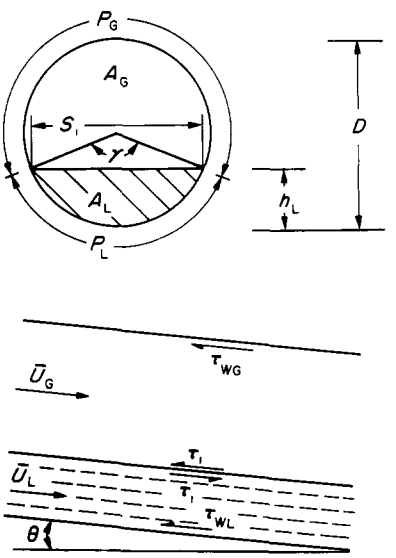

Figure 1. Model of the flow.

acceleration due to gravity and θ is the angle between the pipe and the horizontal; subscripts G and L are for gas and liquid, respectively, i for interfacial and W for wall.

The flow model is shown in figure 1. In [1] and [2] the wall stresses τ_{WL} and τ_{WG} are evaluated by

$$\tau_{WL} = \tfrac{1}{2} f_L \rho_L u_L^2 \qquad [3a]$$

and

$$\tau_{WG} = \tfrac{1}{2} f_G \rho_G u_G^2, \qquad [3b]$$

where u is the phase mean velocity, and the friction factors, f_L and f_G, are the same functions of the liquid and gas Reynolds numbers as in single-phase flow, with Re_L and Re_G defined as

$$Re_L = \frac{4A_L}{P_L} \frac{u_L}{\nu_L} \qquad [4a]$$

and

$$Re_G = \frac{4A_G}{P_G + S_i} \frac{u_G}{\nu_G}. \qquad [4b]$$

In [4a,b] ν is the phase kinematic viscosity.

There have also been attempts at a more rigorous analysis of the flow in the liquid (Buffham 1968; Russel *et al.* 1974; Cheremisinoff & Davis 1979; Shoham & Taitel 1984).

The results obtained by these authors give some improvement in the prediction of stratified flow in a pipe, but the use of [3a] is sufficient for most applications.

In order to predict the interfacial shear stress in [1] and [2] a number of different assumptions or correlations have been used:

1. Johanessen (1972) and Taitel & Dukler (1976) proposed that the film could be considered as a smooth surface for which [3b] applies.
2. Cheremisinoff & Davis (1979) used

$$\tau_i = \tfrac{1}{2} f_i \rho_G u_G^2 \qquad [5]$$

with

$$f_i = 0.008 + 2.00 \cdot 10^{-5} Re_L. \qquad [6]$$

Equation [6] was derived by Miya *et al.* (1971) from data relative to flow in a channel at low liquid Reynolds numbers.

3. Shoham & Taitel (1984) proposed the use of a constant interfacial friction factor, $f_i = 0.0142$, equal to the value found by Cohen & Hanratty (1968) for flow in a channel at low gas velocities.

As can be seen, none of these correlations is based on direct measurements of pressure drops and liquid height relative to flow in a pipe. The scope of the present research is to develop a design method based on actual measurements of main flow parameters. For this purpose, the influence of the interfacial structure on the flow behaviour of the gas and the liquid phases has been carefully examined.

EXPERIMENTAL

The experiments have been conducted in the Two-phase Flow Loop of the University of Trondheim described in detail by Persen (1985). The loop consists of a 26 m long, almost horizontal part terminating in a 10 m high vertical riser. Working fluids are water and air at atmospheric pressure and the pipe i.d. is 5 cm. In these experiments the riser has been disconnected in order to avoid large pressure fluctuations which occur in the horizontal line when churn or slug flow is established in the riser.

The inclination of the pipe can be adjusted with a precision of $<0.02°$. Present experiments are relative to inclinations or 0.65° and 2.1°.

Air and water to the pipe are metered using calibrated rotameters.

In a set of measurements the viscosity of the liquid has been changed by adding glycerine to the water. The viscosity of the water–glycerine solution has been determined by a calibrated viscosimeter.

Pressure drops have been measured close to the outlet from the pipe, using an inclined manometer connected to pressure taps installed at a distance of about 4 m on the top of the pipe.

Film thickness has been measured by the wire probe method, described in detail by Brown *et al.* (1978). In these experiments, two stainless-steel wires, 0.2 mm dia, placed at a distance of 5 mm have been used. The conductance of the wire probe was a linear function of the liquid layer for the full range of values of h_L/D.

The impedance of the probe was measured at 500 kHz using a HP 4815A RF vector impedance meter. In all the experiments the phase of the impedance was about zero and any undesired double-layer effect could be avoided. The analogue output from the impedance meter was converted into a digital signal and analysed by an HP 9845B computer which calculated the first four statistical moments of the signal.

Velocity profiles in the gas phase were measured by a Pitot tube, 1.7 mm dia, which could be very precisely positioned along the axis of symmetry of the pipe cross-section by a micrometer head.

FLOW DESCRIPTION

The flow map has been determined by visual observation of the different flow patterns. In no case were annular flow conditions reached. At high gas velocity some liquid entrainment by the gas was observed.

A few tests with a sampling probe indicated that under the present experimental conditions liquid entrainment was always $<5\%$ of the total liquid flow.

The present research is limited to the study of stratified flow. As shown in figure 2, within this flow regime, the interfacial structure undergoes substantial changes, and at least three different subregimes can be identified:

1. The stratified smooth regime in which the interface may present low-amplitude disturbances, which do not affect the interfacial friction factor.
2. The 2-D wave regime, in which the interface is covered by a continuous 2-D wave structure, observed by the conductance probe, with typical amplitudes of the order 1–2 mm and wavelengths of 10–20 mm. The transition to this flow regime causes a sharp increase in the interfacial friction factor.

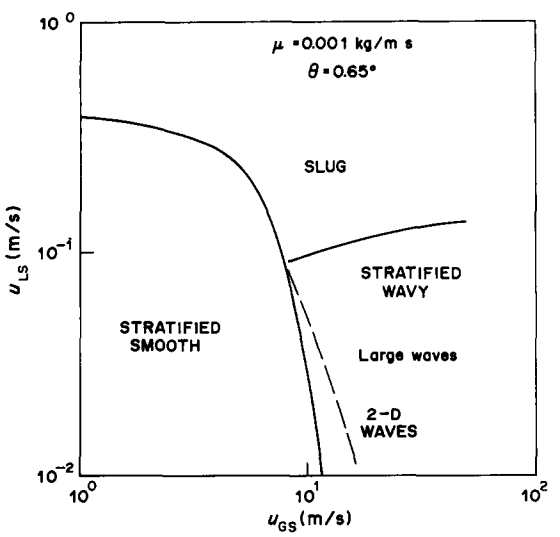

Figure 2. Flow regime map.

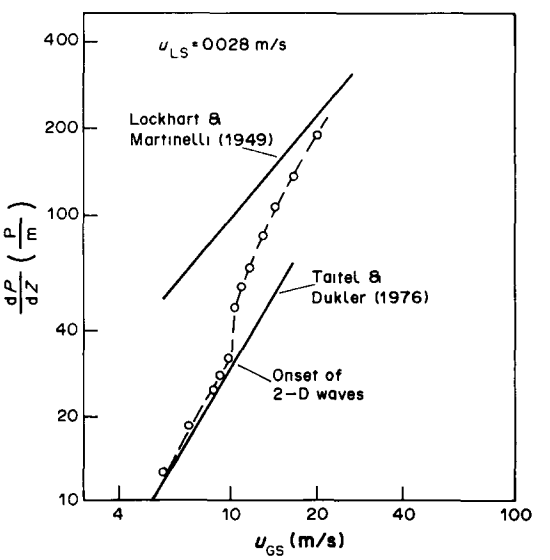

Figure 3. Pressure gradient at the transition to 2-D waves ($\mu_L = 0.001$ kg/s m, $\theta = 0.65°$).

3. The large disturbance wave regime in which large disturbances, observed by a number of authors [see, for instance, Hanratty & Hershman (1961)] are superposed on the 2-D wave structure.

As also shown in figure 2, at high liquid loads, stratified flow is delimited by the transitions from stratified smooth and from the large wave regime to the slug flow regime.

The main features of the flow map determined in the present research are similar to other maps in common use in engineering applications, like those proposed by Mandhane *et al.* (1974) or by Taitel & Dukler (1976). However, a number of important differences can be noticed. The transition from large disturbance waves to slug flow occurs at lower liquid flow rates than predicted by Taitel & Dukler (1976). According to these authors, this transition occurs for $h_L/D \geqslant 0.5$. The present experiments are correlated by the equation $h_L/D \cong 0.25$. Present observations also show that, at high liquid loads, when the gas velocity is gradually increased, it is possible to observe at the same gas velocity the transition to 2-D waves close to the liquid inlet, the transition to large waves a few meters after, and the transition to slug flow close to the outlet. This last transition would not have been observed in a shorter pipe. These observations indicate that the growth of a slug is caused by the same mechanism which produces large waves superposed on a 2-D wave structure.

Moreover, for $h_L/D \geqslant 0.25$ the transition from stratified smooth to the 2-D wave regime appears to coincide with and to determine the transition to slug flow. It follows that, at least under the present experimental conditions, it is sufficient to predict the transition to the 2-D wave regime in order to determine also the onset of slug flow for $h_L/D \geqslant 0.25$.

TRANSITION TO STRATIFIED WAVY FLOW

The transition from stratified smooth to stratified wavy flow causes a large, sharp increase in the pressure gradient. This is shown in figure 3, where measured values of the pressure gradient are compared with the predictions derived according to the design methods proposed by Taitel & Dukler (1976) and by Lockart & Martinelli (1949).

It can be noticed that these two methods give rather different results, but describe reasonably well experimental measurements in the limiting cases of low (Taitel & Dukler) and high (Lockart & Martinelli) gas flow rates.

Interfacial friction factors obtained from pressure-drop measurements are represented in figure 4 as the ratio f_i/f_G vs u_{GS}. As already mentioned, in the stratified smooth regime $f_i \cong f_G$, while at the onset of 2-D waves f_i becomes much larger than f_G and increases with the gas velocity. These features of the stratified smooth to 2-D wave transition allow a very precise identification of the transition line.

In figure 4 the correlation proposed by Hanratty & Andritsos (1984) for friction factors in horizontal flow is also represented. In these experiments the transition from smooth to wavy flow occurs at a much lower gas velocity (1.5 m/s) than in the present work. This velocity appears to be independent of the liquid flow rate. According to Hanratty & Andritsos (1984), f_i/f_G is given by

$$\frac{f_i}{f_G} = 1 \quad \text{for} \quad u < 1.5 \text{ m/s} \qquad [7a]$$

and

$$\frac{f_i}{f_G} = 1 + 0.75\left(\frac{u_{GS}}{1.5} - 1\right) \quad \text{for} \quad u_{GS} > 1.5 \text{ m/s}. \qquad [7b]$$

The differences between horizontal and inclined flows are probably due to the presence of other types of interfacial instabilities in horizontal flow which occur at lower gas velocities. These instabilities may cause a more gradual change in the interfacial structure and in the interfacial shear stress than observed in our experiments.

The transition to large waves, which is very important in vertical flow and at high gas velocity, as in such cases it coincides with the onset of heavy entrainment, does not cause significant modifications to the interfacial stress.

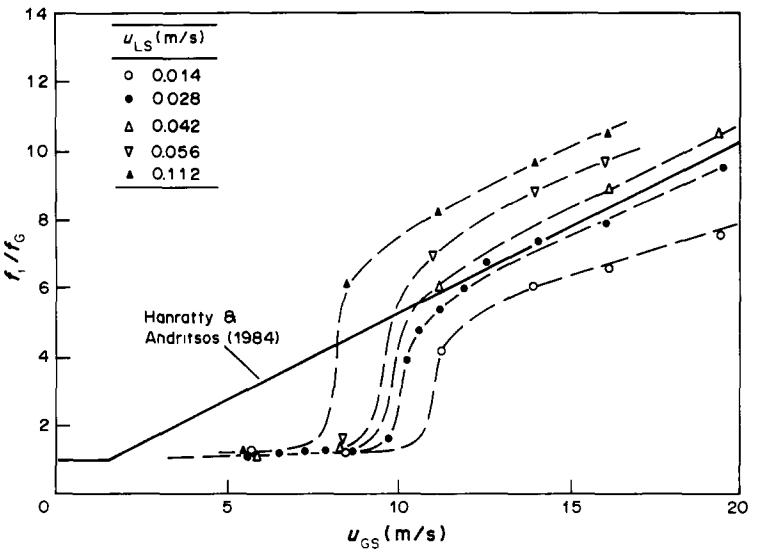

Figure 4. Interfacial friction factors in the 2-D wave regime. Comparison with the correlation of data relative to horizontal flow ($\mu_L = 0.001$ kg/s m, $\theta = 0.65°$).

In order to determine the boundaries of the stratified smooth flow regime, the linear stability analysis proposed by Hanratty & Hershman (1961), and recently also adopted by Andreussi *et al.* (1985), may be the appropriate tool. Unfortunately, this analysis is rather complicated and the results have not been expressed using a simple equation.

This analysis can be drastically simplified when inertia terms in the liquid momentum balance equation are neglected. This approach has been followed by Wallis & Dobson (1973) and Taitel & Dukler (1976). In this case the stability criterion for flow in a channel is given by

$$u_G > \left(g \frac{\rho_L - \rho_G}{\rho_G} h_G \cos\theta \right)^{\frac{1}{2}}, \qquad [8]$$

where h represents the height of the phase cross-section.

For flow in a pipe, [8] can be modified into

$$u_G > \left(\frac{\rho_L - \rho_G}{\rho_G} g \cos\theta \frac{A_G}{\frac{dA_L}{dh_L}} \right)^{\frac{1}{2}}. \qquad [9]$$

As a consequence of the approximations made, it is necessary to introduce an adjustable constant in [8] and [9] in order to fit the experimental data. It can then be expected that the resulting equation will only hold for a limited range of flow variables.

As shown in figure 5, the present results relative to two inclinations and two liquid viscosities are fairly well correlated assuming that the transition occurs at a constant value of the dimensionless number F, defined as

$$F = u_G \left(\frac{\rho_G}{\rho_L - \rho_G} \frac{\frac{dA_L}{dh_L}}{A_G} \frac{1}{g \cos\theta} \right)^{\frac{1}{2}}. \qquad [10]$$

Wallis & Dobson (1973) and Taitel & Dukler (1976) adopted a similar criterion to represent the transition from stratified wavy to slug flow. It may be useful to remark that [10] represents the boundary of the stratified smooth regime and that the linear stability analysis can be, in this case, correctly applied to a smooth interface.

The value of F determined in the present research, $F = 0.44$, is only slightly lower than the value proposed by Wallis & Dobson (1973), $F = 0.5$, for the transition to slug flow in a horizontal channel. This difference and the scatter of data shown in figure 5 is related to minor effects on the transition of the liquid viscosity and the pipe inclination, which may eventually be better described by a more rigorous stability analysis.

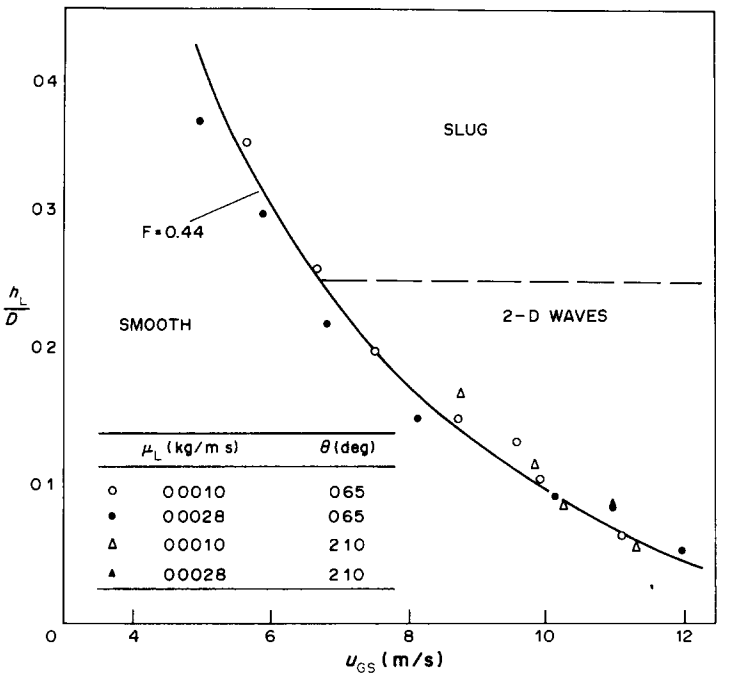

Figure 5. Correlation of flow transitions.

FLOW IN THE GAS PHASE

The present measurements of pressure drop and film thickness have been analysed by means of [1] and [2]. In order to obtain τ_i from [1] it has been assumed that the mean shear stress at the wall relative to the gas phase, τ_{WG}, can be calculated by the same equation used for single-phase flow, [3b], with Re_G given by [4b]. This procedure appears reasonable when $\tau_i \cong \tau_{WG}$, but the use of a gas Reynolds number as defined in [4b] may be questionable when $\tau_i \gg \tau_{WG}$, as in this case the gas flow perimeter does not present a uniform roughness.

The present experimental analysis is heavily dependent on the assumptions made for predicting τ_{WG}. Velocity profiles in the gas phase have then been determined by Pitot tube measurements in order to verify these assumptions, and also to obtain a better insight into the mechanism of momentum transfer at the gas–liquid interface.

In figure 6, three of these velocity profiles are shown, one of which is relative to the case of gas flow only, the other two are for different values of u_{LS} and the same value of u_{GS}. The profiles have been determined along the axis of symmetry of the pipe cross-section.

An interesting feature of these profiles is the progressive displacement of the maximum velocity towards the liquid layer at increasing values of h_L/D. In channel flow, an opposite behaviour has been observed by Cohen & Hanratty (1968), Akai *et al.* (1981) and Fabre *et al.* (1983). Fabre *et al.* also identified a secondary flow pattern which was directed, at the centre of the channel, from the liquid layer to the top of the channel. According to these authors, the shift of the maximum velocity toward the upper wall was related to the presence of secondary flows. In pipe flow the secondary flow appears to be directed in the opposite direction and the shift of the maximum velocity observed in present experiments can actually represent a measure of the magnitude of the secondary flow pattern.

The shear stresses τ_{WG} and τ_i can easily be determined from the velocity profiles if it is assumed that close to the wall and to the gas–liquid interface the law of the wall equations can be adopted to describe the turbulent gas flow. Unfortunately, extensive use of this method to determine τ_{WG} or τ_i is rather tedious. Besides, the presence of droplets at large gas and liquid flows does not allow reliable Pitot tube measurements of the gas velocity.

Therefore, the present measurements of gas velocity have been mainly used to check, for a limited number of cases, the method adopted to obtain τ_{WG} and τ_i from pressure-drop and liquid-height measurements. For this purpose, velocity measurements relative to the wall region have been made

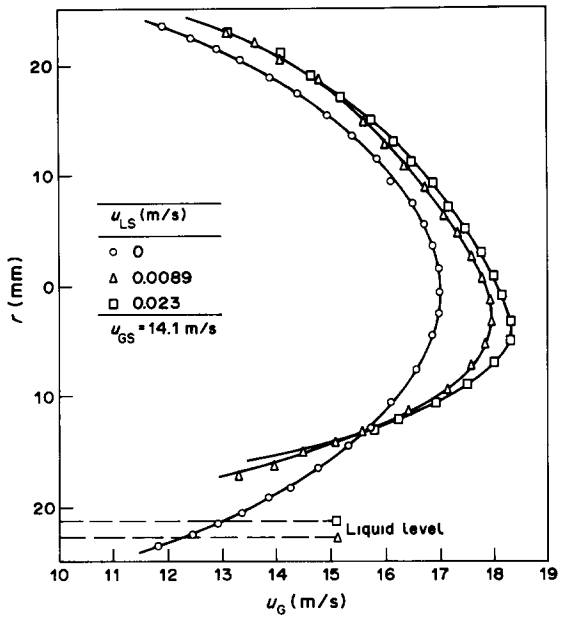

Figure 6. Velocity profiles in the gas phase ($\mu_L = 0.0028$ kg/m s, $\theta = 0.65°$).

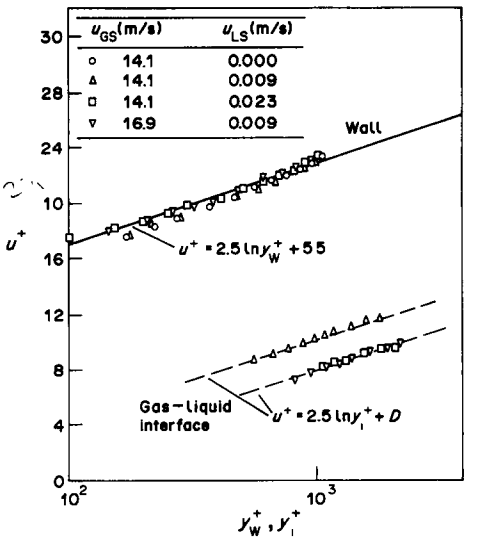

Figure 7. Comparison of velocity profiles with the law of the wall equations ($\mu_L = 0.0028$ kg/m s, $\theta = 0.65°$).

dimensionless with respect to the wall friction velocity,

$$u_W^* = \sqrt{\frac{\tau_{WG}}{\rho_G}}, \qquad [11]$$

and the measurements taken close to the gas–liquid interface with respect to the interfacial friction velocity, u_i^*, defined as

$$u_i^* = \sqrt{\frac{\tau_i}{\rho_G}}. \qquad [12]$$

Length scales have been chosen accordingly. In [11] and [12], τ_{WG} and τ_i are the shear stresses evaluated from pressure-drop and liquid-height measurements.

In figure 7 it is shown that the profiles determined close to the pipe wall are in a very good agreement with the law of the wall equations (see Schlichting 1960):

$$u_W^+ = \frac{u_G}{u_W^*} = 2.5 \ln y_W^+ + 5.5, \qquad [13]$$

where y_W^+ is the dimensionless distance from the wall. The profiles determined close to the liquid layer follow the equation

$$u_i^+ = \frac{u_G}{u_i^*} = 2.5 \ln y_i^+ + D_i, \qquad [14]$$

where, as in rough pipe flow, the constant D_i is found to depend on the interfacial roughness.

The results reported in figure 7 confirm that the wall stress in the gas phase can be correctly calculated by means of [3b]. The interfacial stress can then be derived from [1] and measured values of pressure drop and liquid height.

Dimensionless velocity profiles relative to the gas–liquid interface also suggest that an analogy can be established between flow over a wavy liquid layer and flow in a rough pipe. In particular, the present experiments indicate that the slope of u_i^+ vs $\ln y_i^+$ is equal to the inverse of the von Karman constant, i.e. the same value as in law of the wall equations for flow over a rough surface. Cohen & Hanratty (1968) found that this slope was appreciably higher and concluded that the mechanism of turbulent energy transfer at the gas–liquid interface was different from the case of a rough wall. Their experiments were relative to the case of a horizontal channel, lower gas velocities and a 3-D wave structure.

Table 1

u_{LS} (m/s)	u_{GS} (m/s)	$\frac{k_s u_i^*}{\nu_G}$	$\frac{f_i}{f_G}$	$\frac{h_L}{D}$
0.0089	14.1	520	4.24	0.0475
0.0089	16.9	1256	5.91	0.0375
0.023	14.1	1207	6.52	0.0670

$\mu_L = 0.0028$ kg/m s, $\theta = 0.65°$.

In analogy with flow in a rough pipe, the constant D_i in [14] can be evaluated from experimental measurements and related to the equivalent sand roughness, k_s, by (see Schlichting 1960)

$$D_i = 8.5 - 2.5 \ln \frac{k_s u_i^*}{\nu_G}. \qquad [15]$$

As shown in table 1, the values of the dimensionless number $k_s\, u_i^*/\nu_g$ determined in the 2-D regime are always within the so-called fully rough regime for flow in a rough pipe, i.e. $k_s\, u_i^*/\nu_G > 70$. It can then be expected that the interfacial friction factor f_i be a function of the ratio k_s/R_{Hi}, where R_{Hi} is the hydraulic radius for flow over the wavy interface. It can be assumed that R_{Hi} scales as the distance between the maximum gas velocity and the liquid layer. The limited number of velocity profiles analysed in the present work indicates that this distance is mainly a function of h_L/D. It is also assumed that the size of the interfacial roughness, made dimensionless with respect to the pipe diameter, is a function of the difference $F - F_0$ between the actual value of the Froude number F and its value at the onset of 2-D waves, and eventually of the ratio h_L/D. It is concluded that the interfacial friction factor f_i can be represented as a function of $F - F_0$ and $h_L D$. As for $F = F_0$, $f_i \cong f_G$, it is convenient to express f_i as

$$\left.\begin{aligned} \frac{f_i}{f_G} &= f\left(F - F_0, \frac{h_L}{D}\right) \quad F > F_0 \\ \frac{f_i}{f_G} &= 1 \quad F \leqslant F_0. \end{aligned}\right\} \qquad [16]$$

In figure 8 measured values of f_i/f_G are plotted vs the dimensionless group $(F - F_0)(h_L/D)^{0.3}$. This group, with $F_0 = 0.36$, gives the best fit to the present data. As can be seen, the correlation is good, in particular for flow regimes relative to the same value of inclination and viscosity. As the correlation critically depends on the value of F_0, the scatter of data in figure 8 is probably related to minor effects of viscosity and inclination on the transition to 2-D waves, already noticed in figure 5. When more extensive data are available, it will be possible to improve the correlation considering F_0 as a function of fluid properties and inclination.

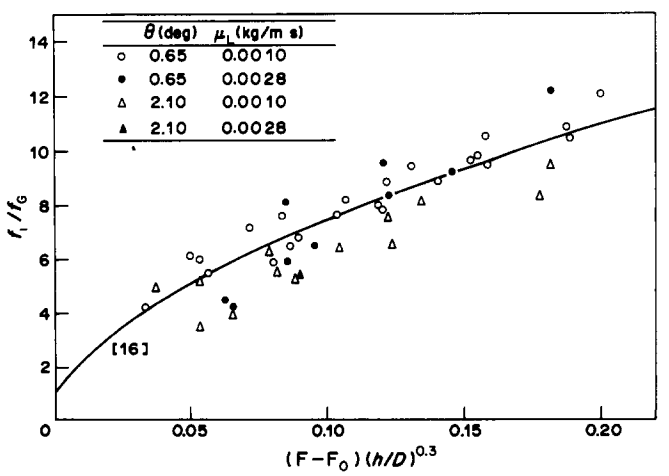

Figure 8. Correlation of f_i/f_G as a function of the dimensionless number $(F - F_0)(h_L/D)^{0.3}$.

Finally, the value of F_0 which gives the best fit to the present measurements of interfacial friction factors ($F_0 = 0.36$) is lower than the value at the transition to 2-D waves ($F_0 = 0.44$). This appears to be mainly due to the fact that the value $F_0 = 0.36$ has been obtained with an optimization procedure applied to an analytical function which presents a jump at $F = F_0$, while experimental measurements show a more gradual variation at the onset of 2-D waves.

The best fit of the data, shown in figure 8, is given by the equation

$$\frac{f_i}{f_s} = 1 + 29.7\,(F - 0.36)^{0.67}\left(\frac{h_L}{D}\right)^{0.2}. \qquad [17]$$

Equation [17] is also represented in figure 8. Due to the limited set of data on which this equation is based, any generalization or the use of [17] for different fluid pairs or flow geometries may lead to appreciable errors.

FLOW IN THE LIQUID PHASE

Simultaneous measurements of the pressure gradient and the height of the liquid layer allow us to derive from [2] the value of the mean shear stress at the wall in the liquid phase, τ_{WL}, when τ_i is calculated from the momentum balance in the gas phase.

The friction factor f_L can be obtained from

$$f_L = \frac{\tau_{WL}}{\frac{1}{2}\rho_L u_L^2}. \qquad [18]$$

In figure 9 experimental values of f_L are plotted vs u_{GS} for a given liquid flow. In the same figure, the values of f_L calculated from the friction factor equation for a smooth pipe,

$$f_L = 0.046\,\mathrm{Re}_L^{-0.2} \qquad [19]$$

with Re_L given by [4a], are also represented. As can be seen from figure 9, at the onset of 2-D waves f_L increases sharply, thus indicating an increase in turbulent dissipation in the film.

At the onset of large waves f_L gradually decreases with increasing u_{GS}. As discussed by Andreussi *et al.* (1985), this behaviour, which is also encountered in the analysis of flow in a channel, can be attributed to the breakdown at the onset of large waves of the assumption of a constant mean liquid film thickness. Large waves move faster than the base film, thus causing a decrease in the mean film thickness and an apparent decrease in dissipation.

All data obtained in the present work show a definite influence of the gas velocity on the friction factor in the liquid. Fortunately, this effect has little consequence on the value of the liquid hold-up, which is a more fundamental parameter in developing design equations. It seems then convenient

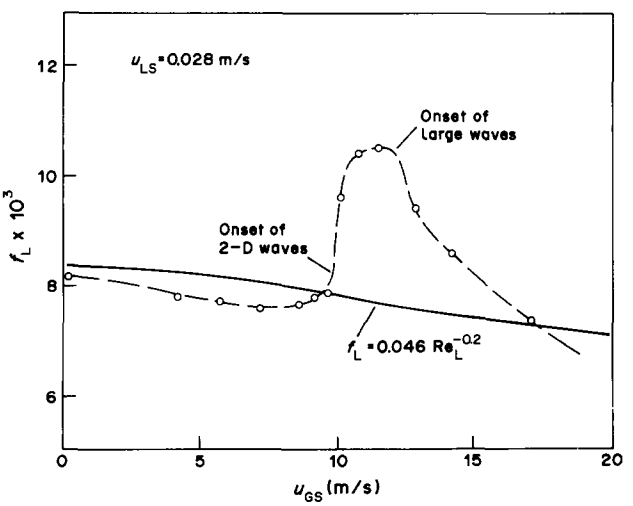

Figure 9. Friction factor at the wall for the liquid phase at the transitions to 2-D waves and large waves. ($\mu_L = 0.001$ kg/m s, $\theta = 0.65°$).

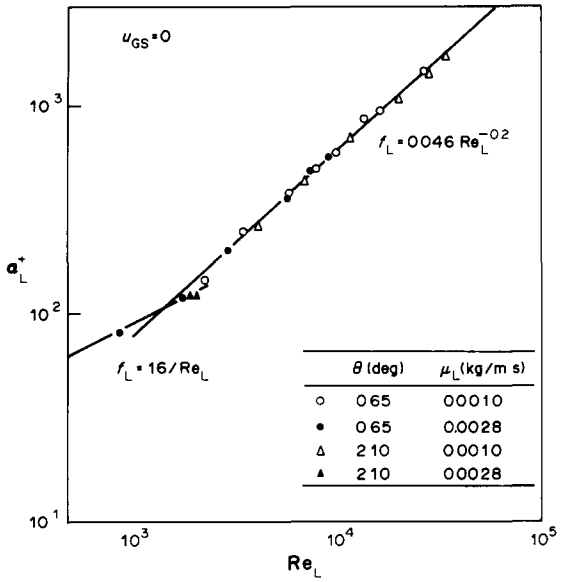

Figure 10. Correlation of α_L^+ vs Re_L for $\mu_{GS}=0$.

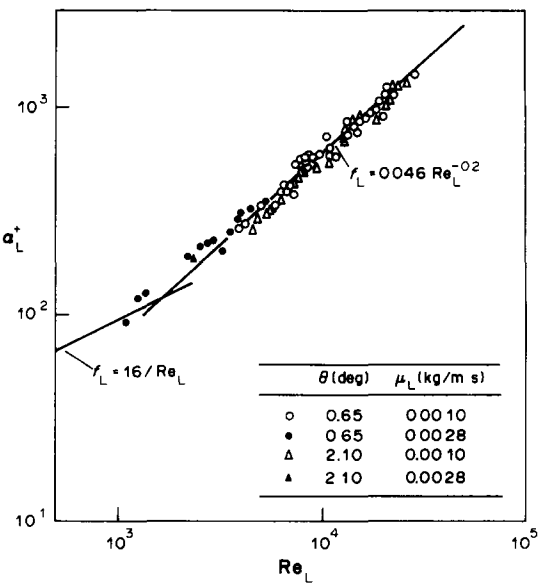

Figure 11. Correlation of α_L^+ vs Re_L for $u_{GS}>5$ m/s.

to derive from [18] a relation between the liquid hold-up α_L and the Reynolds number Re_L, rather than a relation between f_L and Re_L. This can be accomplished by multiplying both sides of [18] by Re_L. After simple manipulations, we obtain

$$\alpha_L^+ = \alpha_L \frac{D}{\nu_L}\left(\frac{\tau_{WL}}{\rho_L}\right)^{\frac{1}{2}} \cdot \frac{\pi D}{P_L} = \left(\frac{f_L}{2}\right)^{\frac{1}{2}} Re_L. \qquad [20]$$

We assume that the r.h.s. of [20] is only a function of Re_L. In figures 10 and 11 we represented measurements of α_L^+ vs Re_L. From figure 10, it can be seen that with no gas flow the theoretical lines which can be predicted assuming laminar and turbulent friction factor relations for single-phase flow are closely followed. As shown in figure 9, in the presence of a turbulent gas, the behaviour of the liquid phase changes but the bulk of the data is still fairly well correlated, assuming that in [20] f_L is given by the same equations as in single-phase laminar or turbulent flow.

CONCLUSIONS

In downwardly inclined pipes the stratified smooth flow regime has a wider extension than in horizontal flow. The transition to a 2-D wave structure occurs with sudden and large modifications of the main flow parameters. At high liquid loads, this transition coincides with and appears to determine the transition to slug flow. The transition to the large disturbance wave regime does not produce significant changes in the flow structure.

The stratified smooth and stratified wavy regimes at low liquid entrainment can be described by simple 1-D models. However, it is necessary to predict correctly the interfacial shear stress.

This is straightforward for the stratified smooth regime, for which it can be assumed that $f_i = f_G$. For the stratified wavy regime, the empirical fit of the present data, [17], can be used along with a trial-and-error procedure.

The velocity profiles in the gas phase can be correlated by the law of the wall equations close to both the pipe wall and the gas–liquid interface. With increasing liquid level, the maximum velocity in the gas phase moves toward the gas–liquid interface.

REFERENCES

ANDREUSSI, P., ASALI, J. C. & HANRATTY, T. J. 1985 Initiation of roll waves in gas–liquid flow. *AIChE Jl* **31**, 119–126.

BROWN, R. C., ANDREUSSI, P. & ZANELLI, S. 1978 The use of wire probes for the measurement of liquid film thickness in annular gas–liquid flow. *Can. J. chem. Engng* **56,** 754–757.

BUFFHAM, B. A. 1968 Laminar flow in open circular channels and symmetrical lenticular tubes. *Trans. Instn chem. Engrs* **46,** 152–157.

CHEREMISINOFF, N. P. & DAVIS, E. J. 1979 Stratified turbulent–turbulent gas–liquid flow. *AIChE Jl* **25,** 48–56.

COHEN, S. L. & HANRATTY, T. J. 1968 Effect of waves at a gas–liquid interface on a turbulent air flow. *J. Fluid Mech.* **31,** 467–476.

FABRE, J., MASBERNAT, L. & SUZANNE, C. 1983 New results on the structure of stratified gas–liquid flow. In *Advances in Two-phase Flow and Heat Transfer* (Edited by KAKAC, S. & ISHII, M.). Nijhoff, The Hague.

HANRATTY, T. J. & ANDRITSOS, N. 1984 Effect of pipe diameter on stratified flow in horizontal pipes. Univ. of Illinois, Urbana, Ill.

HANRATTY, T. J. & HERSHMAN, A. 1961 Initiation of roll waves. *AIChE Jl* **7,** 488–497.

JOHANESSEN, T. 1972 A theoretical solution of the Lockhart and Martinelli flow model for calculating two phase pressure drop and holdup. *Int. J. Heat Mass Transfer* **15,** 1443–1449.

LOCKHART, R. W. & MARTINELLI, R. C. 1949 Proposed correlation of data for isothermal two-phase, two-component flow in pipes. *Chem. Engng Prog.* **45,** 39–48.

MANDHANE, J. M., GREGORY, G. A. & AZIZ, K. 1974 A flow pattern map for gas–liquid flow in horizontal pipes. *Int. J. Multiphase Flow* **1,** 537–553.

MIYA, M., WOODMANSEE, D. E. & HANRATTY, T. J. 1971 A model for roll waves in gas–liquid flow. *Chem. Engng Sci.* **26,** 1915–1926.

PERSEN, L. N. 1984 Stratified two-phase flow in circular pipes. *Int. J. Heat Mass Transfer* **27,** 1227–1238.

PERSEN, L. N. 1985 An experimental study of slug flow in a slightly inclined horizontal pipeline and of disturbance waves appearing in annular flow in vertical risers. In *Proc. 2nd Int. Conf. Multi-phase Flow*, London.

RUSSEL, T. W. F., ETCHELLS, A. W., JENSEN, R. H. & ARRUDA, J. P. 1974 Pressure drop and holdup in stratified gas–liquid flow. *AIChE Jl* **20,** 664–669.

SCHLICHTING, H. 1960 *Boundary Layer Theory*, 4th edn. McGraw-Hill, New York.

SHOHAM, O. & TAITEL, Y. 1984 Stratified turbulent–turbulent gas–liquid flow in horizontal and inclined pipes. *AIChE Jl* **30,** 377–385.

TAITEL, Y. & DUKLER, A. E. 1976 A model for predicting flow regime transitions in horizontal and near horizontal gas–liquid flow. *AIChE Jl* **22,** 47–55.

WALLIS, G. B. & DOBSON, J. E. 1973 The onset of slugging in horizontal stratified air–water flow. *Int. J Multiphase Flow* **1,** 173–193.